J Mater Sci (2023) 58:5086–5103

Polymers & biopolymers

Superhydrophilic bacterial cellulose membranes efficiently separate oil-in-water emulsions

Bhumin Than-ardna[1], Christoph Weder[2], and Hathaikarn Manuspiya[1,*]

[1] *The Petroleum and Petrochemical College, Chulalongkorn University, Bangkok 10330, Thailand*
[2] *Adolphe Merkle Institute, University of Fribourg, Chemin Des Verdiers 4, 1700 Fribourg, Switzerland*

Received: 7 December 2022
Accepted: 3 February 2023
Published online: 3 March 2023

ABSTRACT

Bacterial cellulose (BC) derived from Nata de coco waste was modified and used to develop environmentally friendly superhydrophilic BC membranes with highly efficient oil removal properties. Spherical SiO_2 nanoparticles were synthesized by hydrolyzing tetraethoxysilane (TEOS) in the presence of ammonia and deposited on the surface of the BC membranes to improve their surface roughness and wettability. The modified BC membranes show an efficient water flux ranging from 142 ± 39 to 195 ± 24 $Lm^{-2}\,h^{-1}\,MPa^{-1}$ for oil-in-water emulsions and a separation efficiency of up to 99%. The membranes exhibit good mechanical properties, excellent reusability with high efficiency about 96% after several separation cycles and also good antifouling properties with a higher flux recovery rate (FRR) and reversible fouling ratio (R_r), and a lower irreversible fouling ratio (R_{ir}). Furthermore, the obtained membranes show stability in severe conditions. Thus, the membrane has considerable promise for practical application in the treatment of emulsion wastewater.

Handling Editor: Stephen Eichhorn.

Address correspondence to E-mail: hathaikarn.m@chula.ac.th

https://doi.org/10.1007/s10853-023-08278-w

GRAPHICAL ABSTRACT

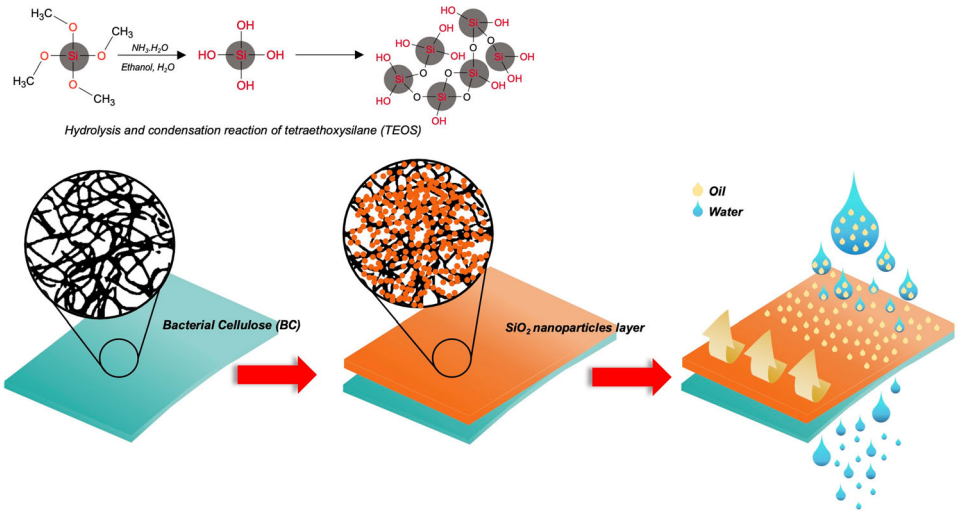

Introduction

Oil-contaminated wastewaters are harmful environmental pollutants that have been a source of concern for many decades [1, 2]. Many industries, including the petrochemical industry, crude oil production, and metal processing facilities, generate significant amounts of oil-contaminated wastewater. The treatment of surfactant-stabilized oil-in-water emulsions that contain oil droplets with diameters of the order of 0.1–20 μm is particularly challenging. Several methods can be used in principle, including electrochemical treatment [3], flocculation [4], and adsorption [5, 6], but they are limited by low efficiency, high energy consumption, and/or secondary pollution.

Membrane technology is an effective and energy-efficient separation method that is a priori ideal for the separation of emulsified oil and water mixtures [7, 8]. Recently, several membranes with suitable wettability and pore size have been developed for this process. In particular, poly(vinylpyrrolidone) (PVP) and poly(ethylene glycol) (PEG) were widely used to increase the hydrophilicity and porosity of asymmetric membranes. It was observed that more than 90% of oil could be effectively captured with the best membranes [9, 10]. Moreover, blends of poly(methyl methacrylate) (PMMA) and PVDF were used instead of the more hydrophobic PVDF in ultrafiltration membranes. It was shown that the hydrophilicity and surface porosity of the membranes increased with the PMMA content, resulting in improved water permeability [11]. Other studies have shown that superhydrophilic membranes with underwater superoleophobicity are generally more suitable for separating oil-in-water (O/W) emulsions, whereas superoleophilic membranes with under-oil superhydrophobicity are preferable for the separation of water-in-oil (W/O) emulsions [12, 13]. Nevertheless, the widespread use of such membranes for large-scale separation is still stifled by limitations such as complex operational processes, high operation costs, high toxicity, poor recyclability and hazardous by-products [14]. Therefore, it is of great importance to research cost-effective and environmentally friendly materials for oil/water emulsion separation.

We propose that some of these problems can be mitigated by separation membranes based on bacterial cellulose (BC) produced by the Acetobacter aceti subspecies xylinum through fermentation of coconut water [15]. This process results in a gelatinous product known as nata de coco, in which the BC adopts a

three-dimensional (3D) nanofibril structure. BC, which is sustainably sourced, is biodegradable and non-toxic to humans and has been widely used as a renewable and functional biomaterial [16, 17] due to its good mechanical properties, low density, and high porosity [18, 19]. Modified BC membranes can be prepared by various methods such as electrospinning, surface grafting, phase inversion, and sol–gel processes [20–23]. Previously, the hydrophilicity of inorganic coatings such as $Cu(OH)_2$ [24], TiO_2 [25], zeolite [26], and especially SiO_2 has been exploited to modify membranes to enhance membrane performance [27]. Jiang et al. added SiO_2 into the PES membrane to improve its permeability and antifouling properties [28], and also, Li et al. coated SiO_2 meshes for separating contaminated oil from corrosive [29]. Recently, Hou et al. reported the deposition of the modified SiO_2 on dried BC membranes with chlorodimethyloctadecylsilane (CDMOS), which was achieved by hydrolysis and condensation [2]. The nanofiber network membranes exhibited a pore size of 0.5–1 μm and underwater superoleophobicity and under-oil superhydrophobicity characteristics that allowed separating W/O emulsions. Moreover, Wahid et al. fabricated bacterial cellulose-based superhydrophilic membranes by blending commercial dopamine hydrochloride with SiO_2 micro-sized particles (SiO_2 MPs) to obtain BC-SiO_2 MPs@PDA composite membranes for O/W emulsion separation [30]. However, MPs can cause an increase in the accumulation of micro-sized particles, possibly causing waste disposal issues in both terrestrial and aquatic environments, including freshwater, sediments, and soil.

BC can be produced with different carbon sources in static and agitated cultures, and its production and structure are affected by several factors such as the types of BC-producing bacterial strains, fermentative media, carbon sources, and growth conditions. These factors can be altered to produce BC with desirable properties [31]. The commercially most relevant product containing BC as a structural component is a gello-like food product known as nata de coco [32]. The waste collected during the manufacturing process contains a considerable amount of BC, and little information is available on the characteristics and functions of BC isolated from such waste. Even though superhydrophilic BC membranes have been reported for O/W emulsion separation, there are still some challenges that need to be more investigated such as different BC sources, complex polymerization methods, anti-oil fouling, durability, mechanical properties, oil/water emulsion separation and especially renewable materials that can be used in wastewater treatment. To our best knowledge, there have been no reports on developing environmentally friendly superhydrophilic BC membranes and separating properties with oil rejection, reusability, pH stability, mechanical properties and anti-oil fouling from bio-based materials from such waste and a few studies have examined the concerning properties of the flux recovery rate (FRR), reversible fouling ratio (R_r), and irreversible fouling ratio (R_{ir}) for emulsified oil/water separation. We show here that a simple and convenient deposition of SiO_2 nanoparticles providing different synthesis approach regarding the development of bio-membranes can be used to transform nata de coco waste from food industries into superhydrophilic membranes that allow a remarkably efficient separation of emulsified oil/water mixtures. Moreover, the SiO_2-modified BC membranes not only demonstrate promising emulsified oil/water separation performance for various oil-in-water emulsions but also offer great recyclability and cost-effective material.

Experimental

Materials

Nata de coco waste was provided by Ampol Food Processing Ltd., Nakorn Pathom, Thailand. Tetraethoxysilane (TEOS) and 25% aqueous ammonia were purchased from Merck Ltd. Ethanol, toluene, petroleum ether and sodium hydroxide 99% were supplied by RCI lab scan Ltd. Sodium chloride was purchased from KEMAUS. Sunflower oil was provided by Thanakorn Vegetable Oil Products Co., Ltd. Essential oil was purchased from local department store, Bangkok, Thailand. Cetyltrimethylammonium bromide (CTAB) was obtained from Tokyo Chemical Industry Co., Ltd. All the chemicals were used as received.

Preparation of bacterial cellulose membrane

500 g of nata de coco waste was cut using a QY-767 blender at ca. 6000 rpm at room temperature. Aqueous NaOH (2%, 2.4 mL per g of slurry) was added and the mixture was stirred at 60 °C for 1 h to remove sugar and impurities. Subsequently, the BC was neutralized

by washing with deionized (DI) water until a pH of 7.0 was reached and the wet BC was isolated by vacuum filtration. After that, 10 g of wet BC was redispersed in 50 mL of DI water and the mixture was homogenized in the QY-767 blender at 30,000 rpm at room temperature for 15 min. This suspension was then processed into a BC membrane by vacuum filtration through a Büchner funnel with a diameter of 6 cm. The membrane was dried at 50 °C for 24 h and had a weight of ca. 0.25 g and a thickness of ca. 74 μm.

Preparation of modified bacterial cellulose membrane—general procedure

The BC membrane was wetted with ethanol before it was immersed for 1 h in 25 mL of a TEOS/ethanol (70:30 v/v) mixture. To hydrolyze and condensate the TEOS and form the SiO_2, the TEOS-treated membrane was then placed into 50 mL of a 10% NH_4OH in ethanol solution (25% aqueous NH_4OH/deionized water/ethanol = 1:1.8:2.75 mL) and ultrasonicated at 25 °C for 30 min. Finally, the membrane was immersed for 1 h in ethanol and for 1 h in water to remove any residual reactants and by-products. The resulting BC-SiO_2 membrane was then dried for 24 h at 50 °C. Parameters that were varied include the immersion time in the TEOS solution, the TEOS/ethanol ratio, the concentration of the NH_4OH solution in ethanol, and the time of the hydrolysis and condensation steps; these data are provided in Table 1.

Preparation of surfactant-stabilized oil-in-water emulsions and separation experiments

The surfactant-stabilized oil-in-water emulsions were prepared by dissolving 100 mg of cetrimonium bromide (CTAB) in 50 mL of water and adding 2 g of oil (toluene, sunflower oil, chloroform, essential oil or petroleum ether) at room temperature. The mixture was stirred for 30 min, followed by sonication for 30 min to obtain stable emulsions, which were used for separation experiments. The separation experiments were carried out by vacuum filtration. The modified BC membranes were clamped between a separation funnel and a vacuum flask (Fig. S1) with an effective area of 12.57 cm^2. 50 mL of the oil-in-water emulsions were poured into the separation funnel and vacuum filtrations were carried out at an operating pressure of 0.088 MPa. The permeation fluxes were measured every 10 min during the separation for 1 h. The flux and oil rejection of the membranes were calculated by Eqs. (1) and (2):

$$Flux = \frac{V}{A \times \Delta t \times P} \tag{1}$$

$$R = \left(1 - \frac{C_p}{C_i}\right) \times 100 \tag{2}$$

where $Flux$ ($Lm^{-2}\ h^{-1}\ MPa^{-1}$) is the membrane flux, V (L) is the volume of filtrate after filtration, A (m^2) is the effective membrane area, Δt (h) is the separation time, and P (MPa) is the operating pressure. R (%) is the oil rejection rate, and C_P and C_i are the concentrations of oil in the permeate and the feed emulsion, respectively.

Reusability and anti-oil fouling

The reusability of the modified BC membranes was evaluated by carrying out five consecutive separation cycles. Thus, 50 mL of oil-in-water emulsion was separated by the modified BC membrane. After that, the modified BC membrane was washed with distilled water and was then reused for separating another 50 mL of oil-in-water emulsion in the next cycle. The flux recovery rate (FRR), reversible fouling ratio (R_r), and irreversible fouling ratio (R_{ir}) were used to examine the anti-oil fouling property of BC-SiO_2 membranes, and these three terms are calculated by Eqs. (3), (4) and (5):

$$FRR = \left(\frac{J_{w,f}}{J_{w,i}}\right) \times 100 \tag{3}$$

$$R_r = \left(\frac{J_{w,f} - J_p}{J_{w.i}}\right) \times 100 \tag{4}$$

$$R_{ir} = \left(\frac{J_{w,i} - J_{w,f}}{J_{w,i}}\right) \times 100 \tag{5}$$

where $J_{w,i}$ ($Lm^{-2}\ h^{-1}\ MPa^{-1}$) is the initial flux of pure water through the BC-SiO_2 membrane, $J_{w,f}$ is the flux of pure water through the cleaned BC-SiO_2 membranes after 5-cycle emulsions filtration, and J_p is the filtration flux of the BC-SiO_2 membrane of the fifth cycle.

Characterization

The functional groups and chemical structure of the BC and BC-SiO_2 membranes were identified by FTIR spectroscopy (Thermo scientific, Nicolet iS5, USA)

Table 1 Reaction parameters and characteristics of BC-SiO_2 membranes

Sample	Immersion time in TEOS (h)	Ratio of TEOS/ Ethanol (v/v)	Ammonia concentration (wt.%)	Hydrolysis/condensation time (min)	Pore size (μm)	SiO_2 particle size (nm)
Neat BC	–	–	–	–	0.62 ± 0.45	–
BC-SiO_2-1	1	30/70	10	30	0.12 ± 0.05	47 ± 10
BC-SiO_2-2	3				0.17 ± 0.06	47 ± 7
BC-SiO_2-3	6				0.16 ± 0.05	80 ± 12
BC-SiO_2-4	12				0.15 ± 0.06	79 ± 12
BC-SiO_2-5	24				0.12 ± 0.04	83 ± 16
BC-SiO_2-6	1	50/50	10	30	0.14 ± 0.04	57 ± 19
BC-SiO_2-7		70/30			0.14 ± 0.04	60 ± 19
BC-SiO_2-8		100/0			0.13 ± 0.09	68 ± 14
BC-SiO_2-9	1	70/30	5	30	0.14 ± 0.04	53 ± 13
BC-SiO_2-10			2		0.15 ± 0.03	50 ± 13
BC-SiO_2-11			1		0.14 ± 0.04	47 ± 13
BC-SiO_2-12	1	70/30	10	20	0.29 ± 0.18	84 ± 20
BC-SiO_2-13				10	0.30 ± 0.13	89 ± 25
BC-SiO_2-14				5	0.22 ± 0.97	90 ± 21

with an iD7 attenuated total reflectance setup. The spectra were measured in the range of 4000–650 cm^{-1} at a resolution of 4 cm^{-1} and a total of 128 scans for each sample. The chemical composition and elemental distribution were further assessed by x-ray photoelectron spectroscopy (XPS) (Kratos, Axis ultra DLD, UK). The morphological properties were investigated by field-emission scanning electron microscopy (FE-SEM) (Hitachi, S-4800, JP). The samples were sputter-coated with platinum for 3 min under vacuum prior to the examination in order to induce particle charging. For each membrane, the dimensions of 100 SiO_2 nanoparticles and 50 pores were extracted from the FE-SEM micrographs using ImageJ software. The water and underwater oil contact angles were measured with a contact angle tester (Kruss, DSA10-Mk2, DE). The composition of samples was observed using energy-dispersive X-ray spectroscopy (EDX) (Hitachi, S-4800, JP) with an acceleration voltage of 20 kV. The surface roughness of membrane with 2 × 2 cm was determined by atomic force microscopy (AFM) (Seiko, SPA400, JP) under trapping mode. The oil-in-water emulsion droplets were analyzed by optical microscopy (Leica, DMRXP, DE). The concentration of oil in the feeds and the filtrates was determined by total organic carbon (TOC) analysis (Shimadzu, ASI-L, JP). The stability of modified membranes was tested in acid solutions with 10^{-1} M HCl (pH 1), 10^{-3} M HCl (pH 3) and 10^{-5} M HCl (pH 5), base solutions with 10^{-5} M

NaOH (pH 9) and 10^{-2} M NaOH (pH 12) and saturated salt solutions with 6.2 M NaCl, respectively. The mechanical properties of as-prepared membranes, including tensile strength, breaking elongation, and Young's modulus, were measured at a stretching rate of 2 mm/min by universal testing machine (Instron, 4206, USA). The membrane is cut into a rectangular shape 10 mm in width × 50 mm in length. In this test, each sample was tested at least five times and then averaged. The modified membranes were immersed into the above-mentioned solutions for 24 h, subsequently washed with DI water, and dried at 50 °C for 24 h. The water contact angles, underwater oil contact angles, and FE-SEM images of the modified membrane after stability tests were investigated to evaluate their stability under the various conditions.

Results and discussion

Membrane preparation and characterization

The fabrication process to produce superhydrophilic BC-SiO_2 membranes is illustrated in Fig. 1. The neat BC membranes were prepared by vacuum filtration of an aqueous suspension derived from nata de coco production waste. The morphology of the membranes was investigated by scanning electron microscopy (SEM). As shown in Fig. 2a, the pristine BC membranes are microporous networks of individual BC fibers and are characterized by an average pore size of 0.61 ± 0.45 µm. The neat BC membranes were immersed in a TEOS/ethanol mixture. The TEOS thus absorbed was subsequently hydrolyzed under catalysis with ammonia and condensed into SiO_2 nanoparticles that decorate the surface of the BC fibers and increase the hydrophilicity of the membranes. The parameters that were varied are the immersion time in the TEOS/ethanol mixture, the ratio of TEOS and ethanol, the concentration of the NH_4OH solution that was used to catalyze the hydrolysis, and the reaction time; these data are provided in Table 1. A first set of modified membranes, denoted as BC-SiO_2-1–BC-SiO_2-5, was prepared by immersing the neat BC membranes for 1, 3, 6, 12, and 24 h, respectively, in a solution with a TEOS/ethanol ratio of 30:70 v/v. The concentration of ammonium hydroxide in the hydrolysis/condensation step (10%) and the reaction time (30 min) were kept constant. SEM images (Fig. 2b–f) reveal that in the BC-SiO_2-1–BC-SiO_2-5 membranes, the BC fibers are densely coated with SiO_2 nanoparticles; in fact, the individual BC fibrils appear to be encased with a layer of SiO_2 nanoparticles, and this led to a considerable reduction in the pore size to 0.12–0.17 µm, independent of the immersion time (Table 1). The average diameter of the individual SiO_2 nanoparticles size was in the range of 47 ± 10–83 ± 16 nm. The data reflect an increased nanoparticle diameter for immersion times in the TEOS solution of 6 h or more, suggesting that the precursor is predominantly *adsorbed* on the BC surface at short immersion times, whereas extended immersion times may lead to swelling of the BC with TEOS. Energy-dispersive X-ray (EDX) spectroscopy mapping was carried out for BC-SiO_2-1 and the data reveal that the surface is composed of C, O, and Si (Fig. 2g, top panel, Table S1), consistent with the fact that silica and oxygen are the constituent elements of the SiO_2

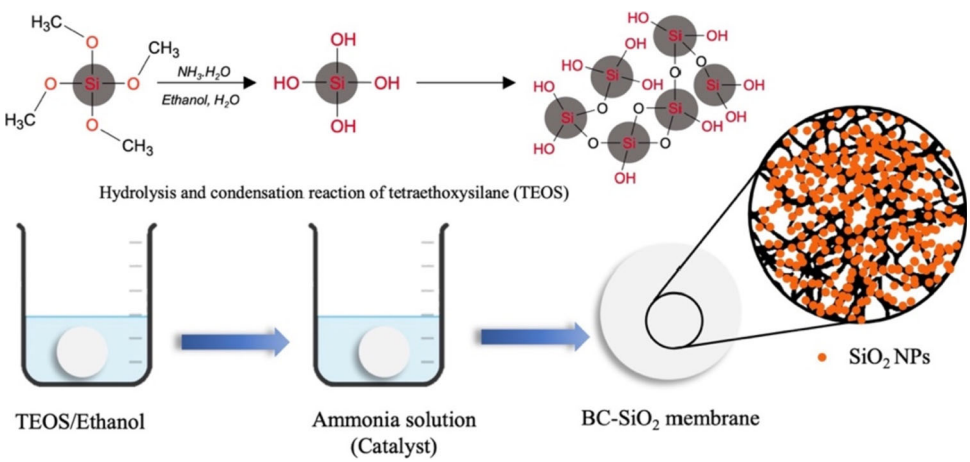

Figure 1 Schematic representation of the process used to prepare the superhydrophilic BC-SiO_2 membranes and the hydrolysis and condensation reactions occurring on the TEOS-coated BC membrane.

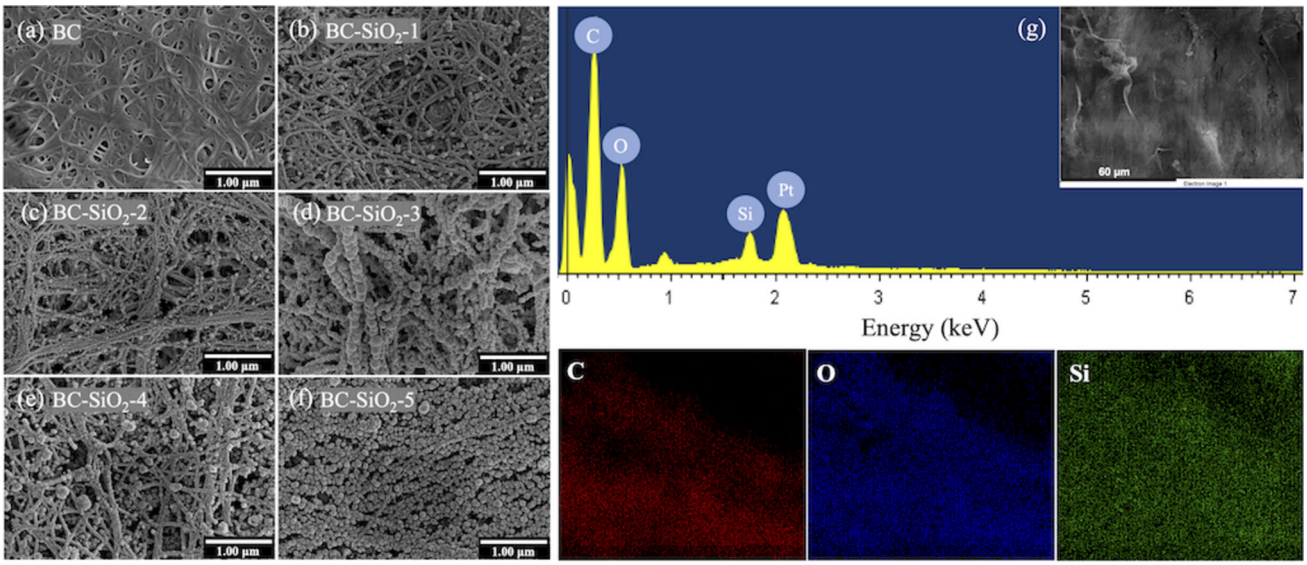

Figure 2 SEM images of **a** the neat BC membrane and the SiO_2 decorated membranes made by varying the immersion time of the neat BC membrane in a solution with a TEOS/ethanol ratio of 30:70 v/v. The concentration of ammonia in the hydrolysis/condensation step (10%) and the hydrolysis time (30 min) were kept constant: **b** BC-SiO_2-1 (1 h), **c** BC-SiO_2-2 (3 h), **d** BC-SiO_2-3 (6 h), **e** BC-SiO_2-4 (12 h), and **f** BC-SiO_2-5 (24 h). **g** EDX spectrum analysis (top) and the element of mapping corresponding C, O, and Si of BC-SiO_2-1 (bottom).

nanoparticles, while carbon is attributed to the structure of BC. The strong Pt signal observed in the EDX is due to the Pt-coating that was applied to the sample for imaging. The mapping of C, O, and Si can be clearly observed as shown in the lower panel of Fig. 2g. The results reveal that SiO_2 nanoparticles are homogeneously distributed on the surface membrane.

The surface chemistries of the BC membrane and the modified BC-SiO_2-1 membrane were probed by ATR-FTIR spectroscopy (Fig. S2). The FTIR spectra of the unmodified BC membrane show a broad peak around 3200−3340 cm^{-1} corresponding to the −OH stretching vibration of hydroxyl groups. Other characteristic signals of cellulose include peaks at 1456 cm^{-1} (asymmetric angular deformation of C−H bond), 1169 cm^{-1} (asymmetric stretching of the C−O−C glycoside bond) and 1050 cm^{-1} (C−OH bond stretching in secondary and primary alcohols). The increased intensity of the peak at 1107 cm^{-1}, which is assigned to Si−OH stretching vibration, and the shifted peak at 887 cm^{-1} in the modified membranes is interpreted with the presence of silanol groups, which are the main source of superhydrophilicity. In addition, new peaks are observed at 1163 cm^{-1} and 1058 cm^{-1}, which correspond to the symmetric stretching vibration of the Si–O–Si and alkyl groups (CH_3), respectively [33]. These results indicated that the surface of precipitated silicas is covered by silanol groups (Si−OH) [34].

We also prepared membranes by following protocols in which the immersion time in TEOS/ethanol was kept constant at 1 h and the other process parameters were varied. When the TEOS/ethanol ratio was increased to 50:50 v/v (BC-SiO_2-6–BC-SiO_2-8, Fig. 3a–c), highly aggregated SiO_2 nanoparticles were found on the surface. Their average diameter (57 ± 19–68 ± 14 nm) was slightly reduced vis a vis the membranes prepared with a lower TEOS concentration, whereas the pore size of the membranes remained unchanged within statistical error. These findings suggest that the ethanol may encourage hydrolysis and condensation, which reduce the efficiency of reactions, resulting in the production of smaller silica nanoparticles [35]. In addition, the ammonia concentration was reduced from 10 to 5%, 2%, or 1% v/v (BC-SiO_2-9–BC-SiO_2-11, Fig. 3d–f). The amount of SiO2 deposited on BC fibers decreases with decreasing ammonia concentration, reflecting that ammonia plays an important role in the hydrolysis and condensation reactions, while the average diameter of the SiO_2 nanoparticles was increased (47–53 ± 13 nm) when the ammonia concentration was increased to 10%. This result indicates

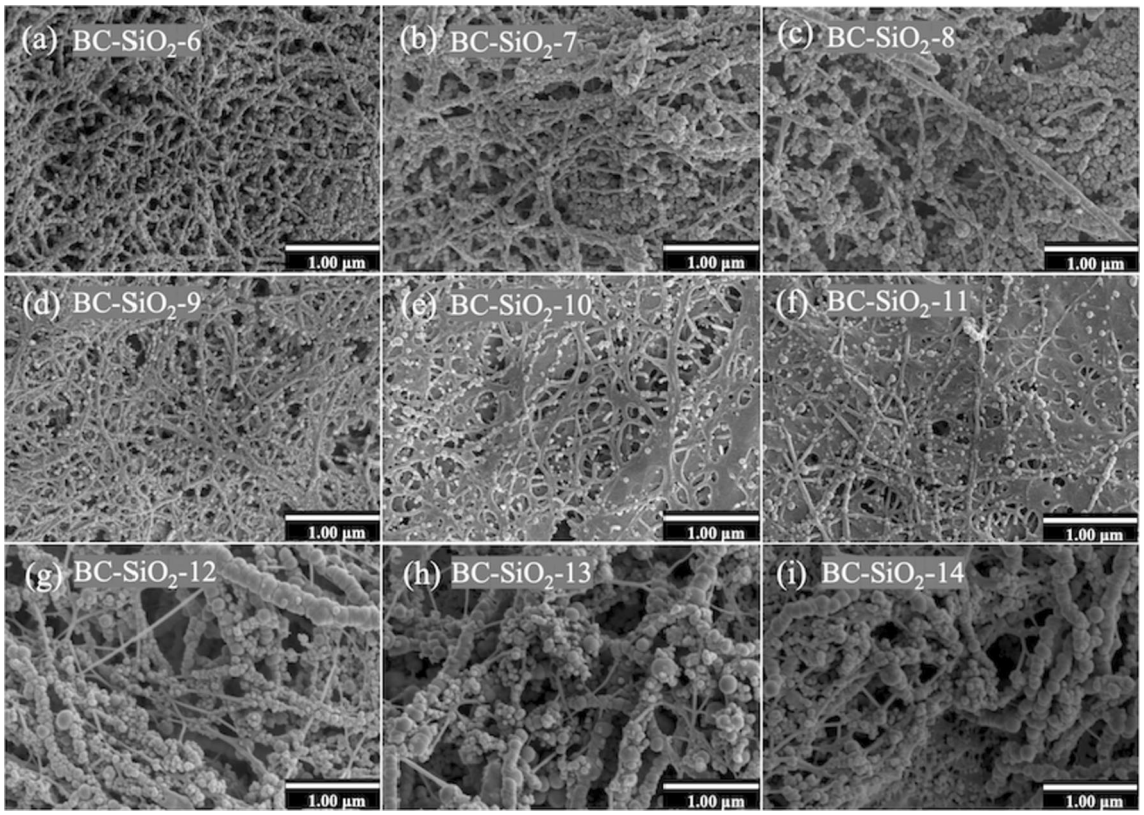

Figure 3 SEM images of BC-SiO2 membrane with the ratio of TEOS/ethanol of **a** 50/50, **b** 70/30 and **c** 100/0 v/v were prepared with an ammonia concentration of 10 wt.% and hydrolysis/condensation times of 30 min, respectively. The ammonia concentrations of (**d**) 1, (**e**) 2 and (**f**) 5 wt.% were prepared with a TEOS/ethanol ratio of 70/30 and a hydrolysis/condensation time of 30 min. The hydrolysis/condensation times of (**g**) 5, (**h**) 10 and (**i**) 15 min were prepared with a TEOS/ethanol ratio of 70/30 and an ammonia concentration of 10 wt.%, respectively.

that the ammonia concentration increases not only the hydrolysis but also the condensation rate, resulting in faster kinetics and greater particle sizes [36], while no obvious influence on the pore size was observed. We also explored conditions in which the ammonia content was kept at 10 wt.% and the hydrolysis/condensation time was varied between 5 and 20 min (BC-SiO_2-12–BC-SiO_2-14, Fig. 3h–i). In this case, the density of SiO_2 particles is irregularly coated and aggregated on the fibers. The average diameter of SiO_2 particles was slightly decreased (84–93 ± 10 nm), indicating that at the initial stage of the hydrolysis and condensation, an interconnected particle network may form, resulting in a small number of large unstable particles on the membrane which affected larger fiber diameters. Therefore, more complete SiO_2 particles have not yet been formed and stable smaller particles may form at a later stage of the process [37]. Moreover, the pore size of the membranes was increased due to the density of SiO_2 formation on fiber entanglements. This parameter is important for the fouling and other characteristics of the membranes. The pore size and distribution of deposited SiO_2 particles may cause the microstructure membrane to achieve superhydrophilic characteristics, which are desirable for oil/water mixture separation, but the smaller the pore diameter, the higher the pressure required for the oil droplets to pass through the membrane. Some of the BC-SiO_2 membranes indeed displayed superhydrophilic/superwetting ($\theta < 5°$–$10°$) characteristics (BC-SiO_2-1–BC-SiO_2-8), whereas others simply displayed hydrophilic ($\theta < 90°$) properties (BC-SiO_2-9–BC-SiO_2-14) (Fig. 4). The water contact angle is dramatically decreased for superhydrophilic/hydrophilic membranes, especially with great distribution of hierarchical SiO_2 nanoparticle structure and high surface roughness. This water can readily be trapped inside the micro- or nanoscale rough surface of the membrane, resulting in a high-

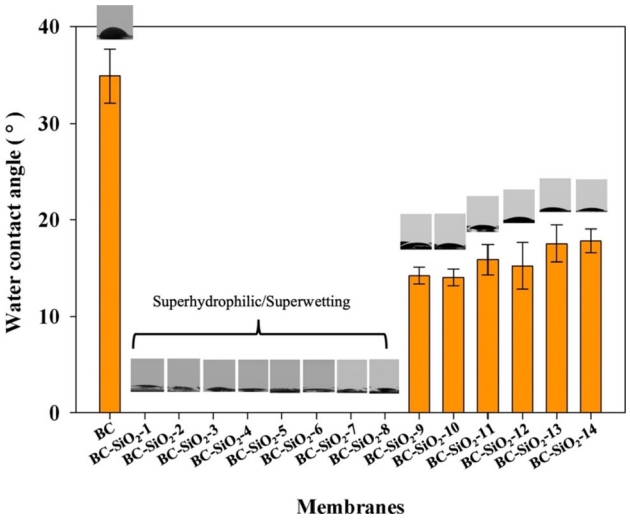

Figure 4 Water contact angles of the pristine BC and the BC-SiO_2 membranes. Pictures were taken 1s after deposition of the water droplet, and angles are reported for the same time.

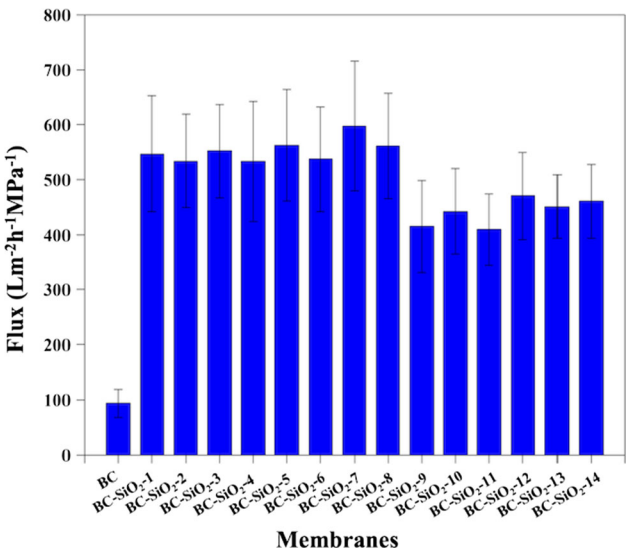

Figure 5 Water flux though the BC and the BC-SiO_2 membranes.

water flux, as demonstrated by the pure water flux of the BC-SiO_2-7 membrane (Fig. 5). It is relevant that modification of superhydrophilic membrane significantly influences high permeation flux with appropriate pore size and wettability. Therefore, the optimal superhydrophilic BC-SiO_2-7, which is synthesized in a 70/30 ratio with an ammonia concentration of 10 wt.% under a reaction time of 30 min, was chosen for further experimentation and discussion in the following section.

To demonstrate the successful hierarchical modification, the pristine BC and BC-SiO_2-7 membranes were analyzed using X-ray photoelectron spectroscopy (XPS). For the pristine BC membrane, the photoelectron peaks characteristic of only carbon and oxygen can be observed in the scan (Fig. S3a). Besides both of these elements, Si was detected on the modified membrane (BC-SiO_2-7), which is deposited as SiO_2 upon the hydrolysis and condensation of TEOS. The deconvoluted high-resolution XPS spectra in the O 1s and Si 2p regions are presented in Fig. S3b-c. The deconvolution of the O 1s spectrum suggests the presence of three components, corresponding to the most intense oxygen atoms of the siloxane groups at 532.3 eV (SiO_2), non-stoichiometric oxides at 531.40 eV (SiO_x), and silanol groups at 533 eV (SiOH), respectively [38]. The presence of SiO2 and Si–OH is considerable at the deposition site and the formation of the Si–OH bond is possibly due to the hydrolysis and condensation of TEOS. Thus, the high concentration of the latter is expected to enhance the hydrophilicity of the membrane. In addition, the Si 2p peak can be deconvoluted into four components, which correspond to the most intense Si–C bonds at 100.53 eV (Si−C), the Si atoms of siloxane groups at 102.88 eV (SiO_2), the shifted Si–O–C bonds and stoichiometry of SiO_x at 99.69 eV, and the shifted elemental silicon at 98.19 eV, respectively [39], confirming again the formation of the expected silicon species.

We also collected higher-resolution SEM and atomic force microscopy (AFM) images of the pristine BC membrane and BC-SiO_2-7 membranes. As shown in Fig. 6a–b, the pristine BC membrane consists of a three-dimensional fibrous network structure that is formed by BC fibrils having a smooth surface. The BC-SiO_2-7 membrane was obviously coated with SiO_2 nanoparticles produced during hydrolysis and condensation, resulting in a much rougher surface (Fig. 6c–d). This is evidenced by AFM results, which show that the average roughness (Ra) of the BC-SiO_2-7 membrane (226.3 nm) was about doubled in comparison with that of the pristine BC membrane (107 nm).

Surface wettability

The wettability of the pristine BC and BC-SiO_2-7 membranes was investigated by water contact angle (WCA) measurements (Fig. 4). As shown in Fig. 7a,

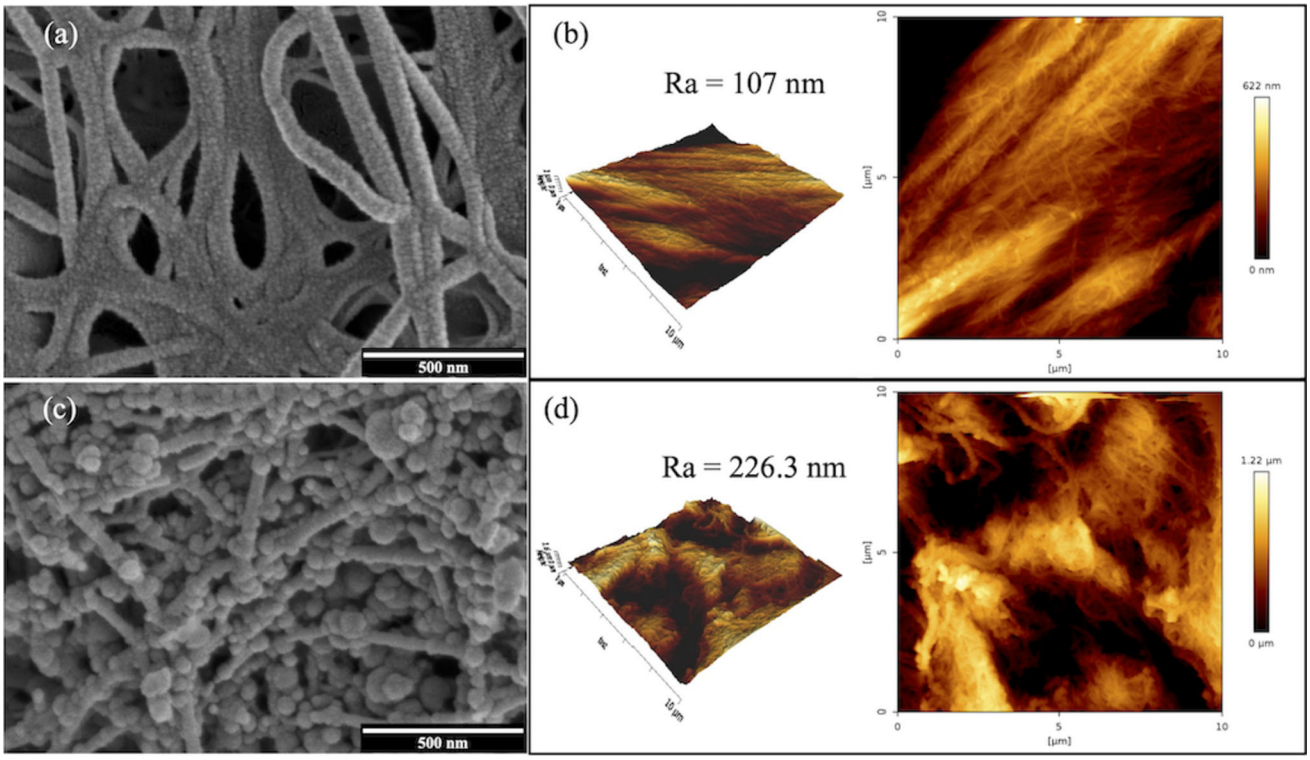

Figure 6 SEM images and AFM graphs of **a**–**b** the pristine BC membrane and **c**–**d** the BC-SiO_2-7 membrane.

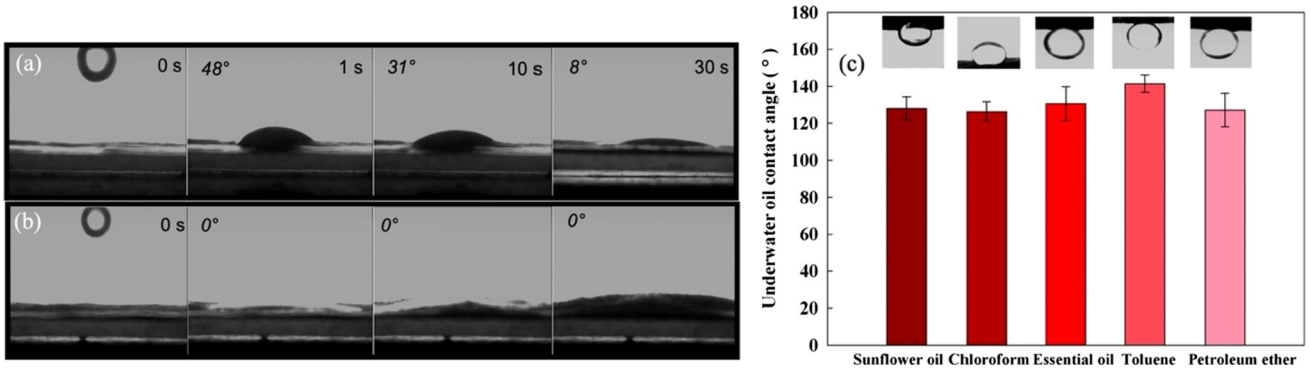

Figure 7 Water contact angle of **a** the pristine BC membrane, **b** the BC-SiO_2-7 membrane and **c** underwater oil contact angle of the BC-SiO_2-7 membrane.

b, the pristine BC membrane exhibited a WCA of about 48°, indicating hydrophilic characteristics that are due to the presence of hydroxy groups on the membrane. The modification with SiO_2 led to an increase in roughness due to the formation of nanoparticles (Fig. 6c) and the formation of silanol groups (Si−OH) contributes to high polarity. As a result, the WCA of BC-SiO_2-7 sharply decreased to about 0°, indicating that the water completely spread across the surface in 1s, and demonstrating the successful transformation of hydrophilicity into superhydrophilicity. The significant change is ascribed to the distinct hierarchical layer-nanosphere coatings with hydrophilic chemical compositions [40]. In addition, we monitored the WCA as a function of time. The WCA of the pristine BC membrane changed over the course of 30 s from 48° to 8°, indicating slow wetting of the porous structure. The BC-SiO_2-7 was immediately wetted and when the duration was prolonged to 30s, considerable swelling was observed as water penetrated through the membrane.

The underwater oil contact angle (UWOCA) of BC-SiO_2-7 was also investigated. As shown in Fig. 7c, the UWOCA was measured for several types of oil, such as sunflower oil, chloroform, essential oil, toluene and petroleum ether, and was always greater than 126°, implying that the modified membrane exhibits good underwater oleophobicity due to its high surface roughness and hydrophilicity [41, 42].

Oil-in-water emulsion separation

On account of the superhydrophilicity and underwater oleophobicity of BC-SiO_2-7, the flux of pure water through this membrane (597 ± 118 Lm^{-2} h^{-1} MPa^{-1}) is much higher than that through the neat BC membrane (94 ± 26 Lm^{-2} h^{-1} MPa^{-1}, Fig. 5), in spite of the much smaller pore size in the latter, which should generally promote a higher water flux [43, 44]. The water flux and separation efficiency of the BC-SiO_2-7 membranes were determined for several types of surfactant-stabilized oil-in-water emulsions, as shown in Fig. 8a. Sunflower oil, chloroform, essential oil, toluene and petroleum ether were used in this study, and we investigated the separation of sunflower oil/water, chloroform/water, essential oil/water, toluene/water and petroleum ether/water mixtures stabilized with a surfactant (CTAB). The average droplet sizes of the various organic oils in the emulsions were in the range of 0.5–18 μm (Fig. S4). The milky toluene-in-water emulsion became transparent after filtration (Fig. 8b–c and Supporting Video 1), and no oil droplets remained in the filtrate without oil/water phase separation (Fig. 8d–e). In the case of sunflower oil-in-water, chloroform-in-water, essential oil-in-water and petroleum ether-in-water emulsion separation, no oil droplets in the filtrate and phase separation of oil and water were observed (Fig. S5). This is due to the high roughness and superwettability of the membrane surfaces which were useful in breaking the emulsion droplets when the emulsion contacted with the membrane surface and repelling oil separation from the highly hydrophilic hydroxyl groups from SiO_2 NPs, as well as hydroxyl groups from BC. This modified BC membrane could readily absorb water molecules and block oil droplets rolling on the membrane surface. However, the residual surfactant which is dissolved in water may be present in the filtrate [40]. The water flux of BC-SiO_2-7 measured for such separations ranged from 142 ± 39 to 195 ± 24 Lm^{-2} h^{-1} MPa^{-1}. In addition, the separation efficiencies for sunflower oil-in-water (98.30%), chloroform-in-water (97.0%), essential oil-in-water (97.23%), toluene-in-water (99.0%), and petroleum ether-in-water (97.19%) emulsions were all higher than 97%. Thus, BC-SiO_2-7 exhibited excellent membrane flux and high separation efficiency toward oil-in-water emulsions.

Reusability and anti-oil fouling property

The reusability of BC-SiO_2-7 membranes was investigated by five repeated separations of toluene-in-water emulsions. As shown in Fig. 9a, the membrane

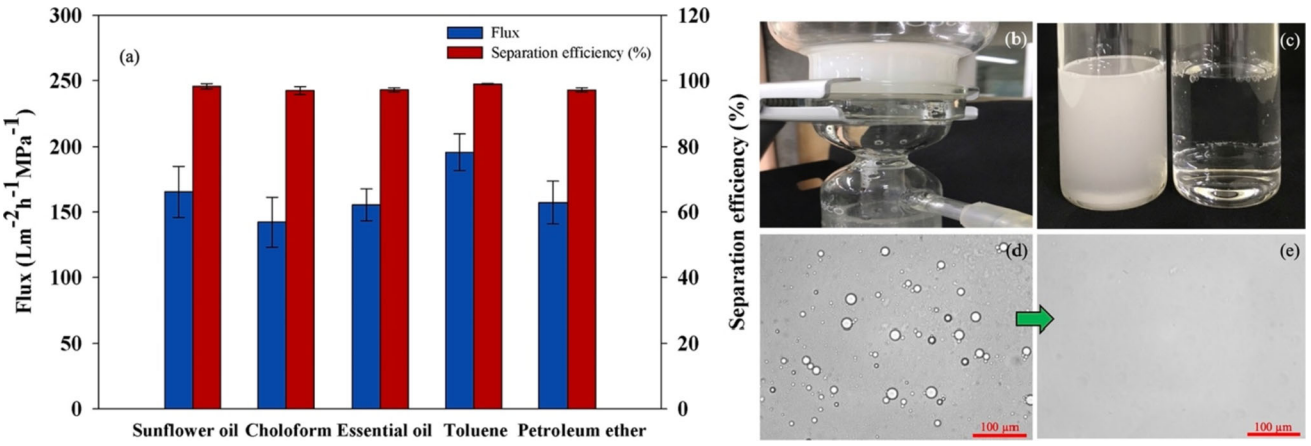

Figure 8 **a** Membrane flux and separation efficiency of BC-SiO_2-7 for different oil-in-water emulsions. **b** Pictures showing the separation of a toluene-in-water emulsion by filtration through a BC-SiO_2-7 membrane. **c** Photograph of the pristine toluene-in-water emulsion (left) and the collected filtrate after filtration (right) through BC-SiO_2-7. (d,e) Optical microscopy images of **d** the pristine emulsion and **e** the collected filtrate. The scale bars are 100 μm.

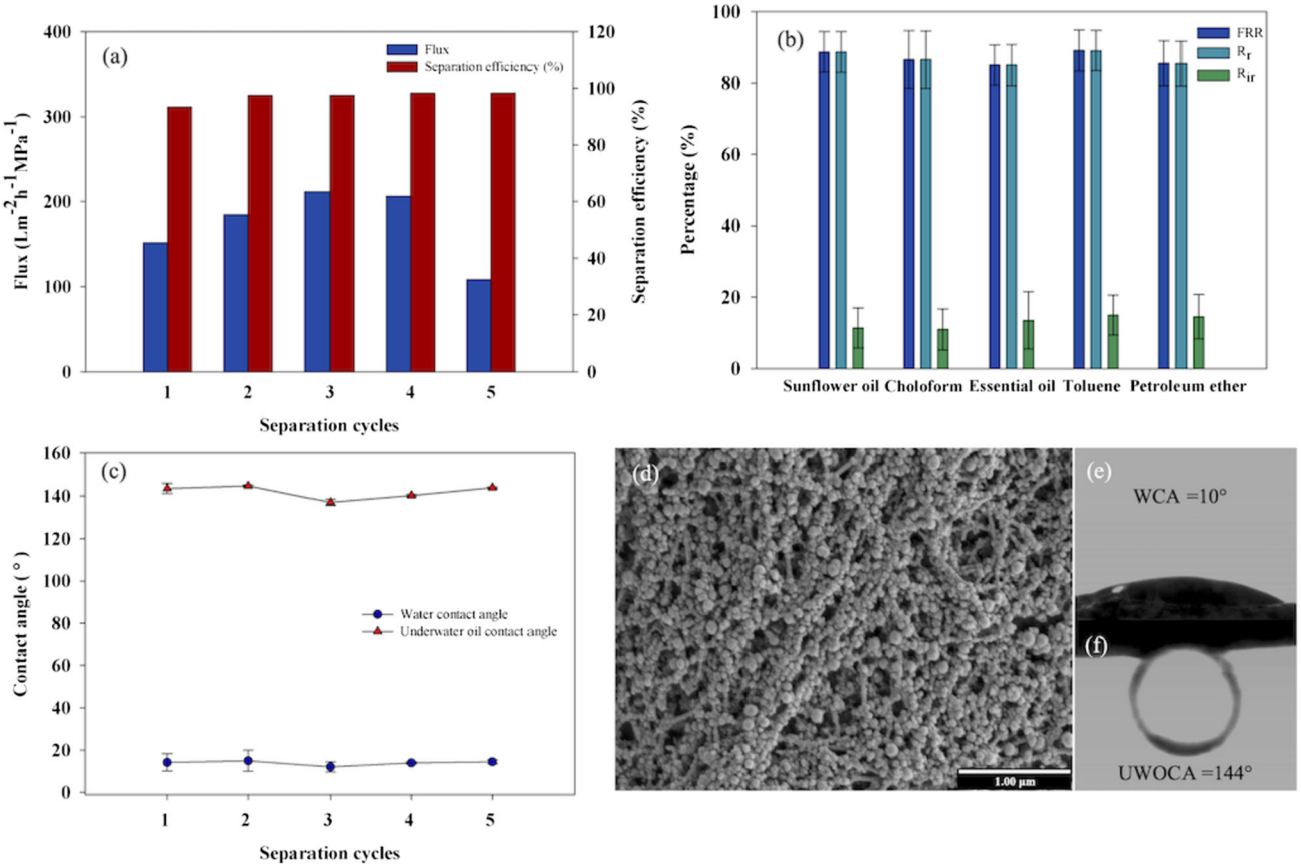

Figure 9 **a** Reusability of BC-SiO_2-7 for the separation of toluene-in-water emulsions. Shown are the flux and separation efficiency for five consecutive separations. **b** Flux recovery rate (FRR), reversible fouling ratio (R_r), and irreversible fouling ratio (R_{ir}) BC-SiO_2-7 for separating different oil-in-water emulsions. Data are after five separation cycles. **c** WCA and UWOCA of BC-SiO_2-7 after separating different cycling test. **d** SEM, **e** WCA and **f** UWOCA images of BC-SiO_2-7 after five separation cycles.

flux of BC-SiO_2-7 first increased, then decreased with the number of separation cycles. This is likely the result of swelling of the membrane during the first cycles, which should increase the permeation, before the deposition of oil droplets causes a reduction in the membrane flux after several separations. However, after five cycles, the membrane flux of BC-SiO_2-7 was still 108 Lm^{-2} h^{-1} MPa^{-1}, and thus comparable to that of the first cycle. Meanwhile, the separation efficiency of BC-SiO_2-7 was hardly affected and remained high efficiency about 96% over five separation cycles.

The anti-oil fouling properties of BC-SiO_2-7 were examined with various oil-in-water emulsions. After the fifth cycle, the BC-SiO_2-7 showed a flux recovery rate (FRR) of > 85%, a reversible fouling ratio (R_r) of > 85%, as well as a low irreversible fouling ratio (R_i) (< 15%) (Fig. 9b). These findings suggest that any absorbed oil droplets on the surface of modified membranes can be removed by simply rinsing the membranes with water and that oil droplet fouling can be reverted for the hydrophilic membranes studied. It appears that the high roughness of the membrane surface was useful in breaking the emulsion droplets and also that the superwettability could promote the anti-oil fouling properties of the membrane. Moreover, the oil droplet, for example, chloroform, was further evaluated. The oil droplet touching the membrane underwater was deformed by pressing down and then gradually removed from the surface of the membrane (Fig. S6). The oil droplet could be easily lifted off the surface of the membrane, indicating that the membrane exhibited good underwater oil resistance. This result was attributed to the abundance of hydroxyl groups with the hydration layers on the membrane surface, which could facilitate water permeation. After five cycles of reusing the filtration process, no obvious change is

observed and abundant nanospheres are still exiting on the membrane surface (Fig. 9c, d). Accordingly, the WCA and UWOCA did not change considerably (Fig. 9e, f).

The comparison of different membranes derived from various raw materials and methods for surfactant-stabilized oil-in-water emulsion separation is summarized in Table 2. The wettability of our BC-SiO_2 membranes and most of other reported membranes were superhydrophilic/hydrophilic to remove oil from emulsions. The pore size of the BC-SiO_2 membranes was in the range of 0.12–0.17 μm, which was sufficiently small to repel oil droplet sizes with particles of 0.5–18 μm. We obtained BC-SiO_2 membranes with the highest oil rejection of 99% and water fluxes ranging from 142 to 195 L^{-1} m^{-2} h^{-1} - MPa^{-1}. The fouling resistance of BC-SiO_2 membrane displayed high FRR, R_r values, and low R_{ir} values for surfactant-stabilized oil-in-water emulsions because the fouling resistance analysis with higher FRR, R_r, and lower R_{ir} generally implies superior anti-oil fouling properties of membranes. These findings were attributed to a hierarchical layer of silicon nanoparticles on BC membranes, which could perform surfactant-stabilized oil-in-water emulsion separations comparable to those of membranes.

Stability and mechanical properties

The stability of the SiO_2 modified membranes was examined using acidic HCl (pH = 1, 3, and 5, respectively), alkaline NaOH (pH = 9 and 12, respectively), and salt NaCl (saturated sodium chloride) solutions. After treatment with the above solutions for at least 24 h, the WCA and UWOCA of the BC-SiO_2-7 membrane remained unchanged, with values of between 0°–14° and 120°–140°, respectively (Fig. 10a) and there was still a superhydrophilic membrane requirement. Furthermore, hierarchical SiO_2 nanosphere structures can be seen in SEM images of the BC-SiO_2-7 membrane after the treatment under different conditions (Fig. 10b–g), and there was no obvious influence on morphology of membrane, indicating the stability of the hierarchical layer-nanosphere coatings. These findings suggest that the BC-SiO_2-7 membrane is robust under a wide range of conditions.

The membrane in practical surfactant-stabilized emulsion separation usually run withstand high hydrostatic pressure or even violent mechanical vibrations from pumps, the mechanical strength of the BC-SiO_2 membranes is important. The mechanical properties of as-prepared BC membranes in terms of tensile strength, elongation at yield and Young's modulus are shown in Table S2. It can be seen that the tensile strength and Young's modulus of pristine BC membranes decreased after modification (BC-SiO_2-7 membranes) ranging from about 39 to 24 MPa, and 2911 to 2075 MPa, respectively. This is due to the aggregation of SiO_2 NPs increasing microstructural dispersion on the membrane surface and acting as stress concentration sites, which decreases the mechanical stability of the membrane. The elongation at break gradually increased from 0.040 to 0.048 mm/mm due to the increased interfacial adhesion between 3D network structure of BC and the decorated SiO_2 NPs.

Conclusion

The BC-SiO_2-7 membrane derived from nata de coco waste was obviously decorated with a hierarchical layer of silica nanoparticles by hydrolysis and condensation processes using this *in situ* method. BC-SiO_2-7 membranes showed successfully superhydrophilicity (almost 0°) and underwater oleophobicity (> 126°) and the rougher BC-SiO_2-7 membrane was found to be beneficial the oil-in-water emulation separation. BC-SiO_2-7 membranes could effectively separate oil-in-water emulsions with the highest oil rejection of 99% and efficient membrane flux. Moreover, BC-SiO_2-7 membranes exhibited good mechanical properties, excellent reusability throughout several filtration cycles, good anti-oil fouling ability and also stability in pH treatment. Thus, this simple method, environmentally friendly and low-cost starting material fabrication process had great

Table 2 Comparison of the comprehensive performance of BC-SiO_2 membranes and other membranes for separation of surfactant-stabilized oil-in-water emulsions reported in literature works

Materials	Bio-based materials	Wettability	Pore size (μm)	Surfactant-stabilized emulsions			FRR (%)	R_r (%)	R_{ir} (%)	Refs.
				Droplet sizes (μm)	Flux ($Lm^{-2} h^{-1}$)	Efficiency (%)				
PVDF-TA membrane	x	Superhydrophilic	~ 0.25	0.32–3.04	56–401 (0.8 bar)	98.0	~ 90*	~ 90*	~ 15*	[45]
PVDF-PDA membranes	x	Hydrophilic	0.46–0.52	< 10*	2600 (1.0 bar)	98.5	91.3	3.2	8.8	[46]
PVDF-BCs/Pd NPs membranes	x	Hydrophilic	~ 0.11	0.1–5	3832 (0.05 MPa)	99.8	–	–	–	[47]
PES-HPAN/SiO_2 NPs membrane	x	Hydrophilic	< 0.25*	~ 0.5*	~ 120* (0.1 MPa)	99.0*	–	–	–	[48]
TCNC-nylon filter membrane	x	Superhydrophilic	0.048–0.07	0.1–0.25*	1036–1734 (0.5 bar)	99.9	–	–	–	[49]
TCNC filter papers	/	Superhydrophilic	0.14–36.2	5–40	43–317 (0.2 bar)	99.1	–	–	–	[50]
All cellulose composite membranes	/	Hydrophilic	< 0.2	~ 1.1	~ 35–45 (gravity)	95.9	–	–	–	[51]
Cellulose nanosheet membranes	/	Hydrophilic	< 0.012	0.2–0.4	1550–1590 (0.8 bar)	98.0	–	–	–	[52]
CNF-$La(OH)_3$ membranes	/	Superhydrophilic	~ 0.28	3.5–9.5*	436.4 (gravity)	98.5	–	–	–	[53]
TCNC-TiO_2 NPs membranes	/	Superhydrophilic	< 0.070	0.15–2	1727 − 1887 (0.5 bar)	99.5	–	–	–	[54]
BC-SiO_2 MPs@PDA composite membranes	/	Superhydrophilic	0.029	0.5–9*	1250 (< 0.1 bar)	98.2	–	–	–	[30]
BC-SiO_2 NPs membranes	/	Superhydrophilic	0.12–0.17	0.5–18	142 − 195 (0.088 MPa)	99.0	> 85	> 85	< 15	This work

*Calculated from figures with datasets

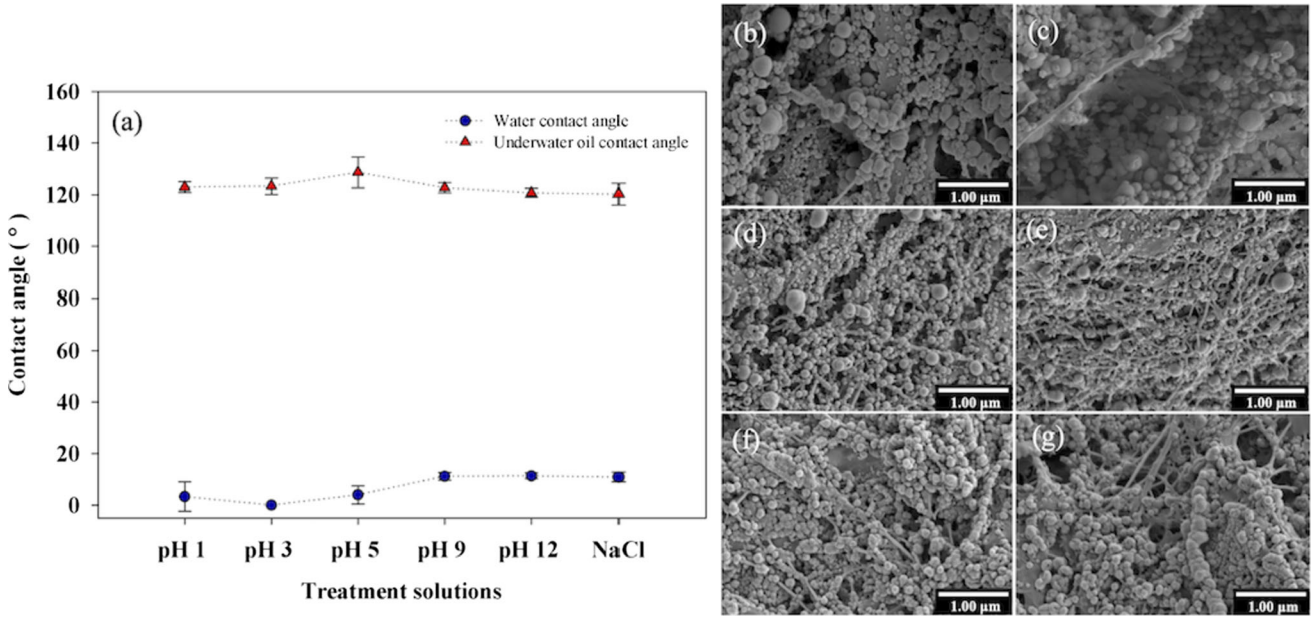

Figure 10 **a** The WCA and UWOCA of the BC-SiO_2-7 after treating with acid, alkaline and salt solutions for 24 h, respectively. The oil used for this test is dichloroethane. **b**–**g** SEM images of the BC-SiO_2-7 after being treated by (**b**) acid (pH = 1), (**c**) acid (pH = 3), (**d**) acid (pH = 5), (**e**) alkali (pH = 9), (**f**) alkali (pH = 12) solutions and (**g**) saturated sodium chloride for 24 h, respectively.

potential for particle use of oil-in-water emulsions in wastewater.

Acknowledgements

This research project is supported by the Second Century Fund (C2F), Chulalongkorn University, Thailand. HM and CW gratefully acknowledge funding from the Swiss National Science Foundation (SNSF) under the SNSF-SPIRIT scheme (Grant No. IZSTZ0_199067 / 1).

Declarations

Conflict of interest The authors declare that they have no conflict of interest.

Ethical approval Not applicable.

Supplementary Information: The online version contains supplementary material available at https://doi.org/10.1007/s10853-023-08278-w.

References

[1] Shannon MA, Bohn PW, Elimelech M, Georgiadis JG, Mariñas BJ, Mayes AM (2008) Science and technology for water purification in the coming decades. Nature 452:301–310. https://doi.org/10.1038/nature06599

[2] Hou Y, Duan C, Zhu G et al (2019) Functional bacterial cellulose membranes with 3D porous architectures: conventional drying, tunable wettability and water/oil separation. J Membr Sci 591:117312. https://doi.org/10.1016/j.memsci.2019.117312

[3] Souza RBA, Ruotolo LAM (2013) Electrochemical treatment of oil refinery effluent using boron-doped diamond anodes. J Environ Chem Eng 1:544–551. https://doi.org/10.1016/j.jece.2013.06.020

[4] Daud Z, Awang H, Latif AAA, Nasir N, Ridzuan MB, Ahmad Z (2015) Suspended solid, color, COD and oil and grease removal from biodiesel wastewater by coagulation and flocculation processes. Procedia Soc Behav Sci 195:2407–2411. https://doi.org/10.1016/j.sbspro.2015.06.234

[5] Kordjazi S, Kamyab K, Hemmatinejad N (2020) Super-hydrophilic/oleophobic chitosan/acrylamide hydrogel: an efficient water/oil separation filter. Adv Compos Hybrid Mater 3:167–176. https://doi.org/10.1007/s42114-020-00150-8

[6] Wang J, Chen Y, Xu Q, Cai M, Shi Q, Gao J (2021) Highly efficient reusable superhydrophobic sponge prepared by a

facile, simple and cost effective biomimetic bonding method for oil absorption. Sci Rep 11:11960. https://doi.org/10.1038/s41598-021-91396-9

[7] Li L, Liu L, Lei J, He J, Li N, Pan F (2016) Intelligent sponge with reversibly tunable super-wettability: robust for effective oil–water separation as both the absorber and filter tolerate fouling and harsh environments. J Mater Chem A 4:12334–12340. https://doi.org/10.1039/C6TA03581G

[8] Gupta RK, Dunderdale GJ, England MW, Hozumi A (2017) Oil/water separation techniques: a review of recent progresses and future directions. J Mater Chem A 5:16025–16058. https://doi.org/10.1039/C7TA02070H

[9] Chakrabarty B, Ghoshal AK, Purkait MK (2008) Ultrafiltration of stable oil-in-water emulsion by polysulfone membrane. J Membr Sci 325:427–437. https://doi.org/10.1016/j.memsci.2008.08.007

[10] Chakrabarty B, Ghoshal AK, Purkait MK (2010) Cross-flow ultrafiltration of stable oil-in-water emulsion using polysulfone membranes. Chem Eng J 165:447–456. https://doi.org/10.1016/j.cej.2010.09.031

[11] Ochoa NA, Masuelli M, Marchese J (2003) Effect of hydrophilicity on fouling of an emulsified oil wastewater with PVDF/PMMA membranes. J Membr Sci 226:203–211. https://doi.org/10.1016/j.memsci.2003.09.004

[12] Wan Z, Xia H, Guo S, Zeng C (2021) Water-in-oil Pickering emulsions stabilized solely by a naturally occurring steroidal sapogenin: Diosgenin. Food Res Int 147:110573. https://doi.org/10.1016/j.foodres.2021.110573

[13] Kota AK, Kwon G, Choi W, Mabry JM, Tuteja A (2012) Hygro-responsive membranes for effective oil–water separation. Nat Commun 3:1025. https://doi.org/10.1038/ncomms2027

[14] Yang H-C, Pi J-K, Liao K-J et al (2014) Silica-decorated polypropylene microfiltration membranes with a mussel-inspired intermediate layer for oil-in-water emulsion separation. ACS Appl Mater Interfaces 6:12566–12572. https://doi.org/10.1021/am502490j

[15] Ajkidkarn P, Manuspiya H (2020) Novel bacterial cellulose nanocrystals/polyether block amide microporous membranes as separators for lithium-ion batteries. Int J Biol Macromol 164:3580–3588. https://doi.org/10.1016/j.ijbiomac.2020.08.234

[16] Huang L, Chen X, Nguyen TX, Tang H, Zhang L, Yang G (2013) Nano-cellulose 3D-networks as controlled-release drug carriers. J Mater Chem B 1:2976–2984. https://doi.org/10.1039/C3TB20149J

[17] Wu ZY, Li C, Liang HW, Chen JF, Yu SH (2013) Ultralight, flexible, and fire-resistant carbon nanofiber aerogels from bacterial cellulose. Angew Chem 125:2997–3001. https://doi.org/10.1002/ange.201209676

[18] Yang X, Cranston ED (2014) Chemically cross-linked cellulose nanocrystal aerogels with shape recovery and superabsorbent properties. Chem Mater 26:6016–6025. https://doi.org/10.1021/cm502873c

[19] Sehaqui H, Zhou Q, Berglund LA (2011) High-porosity aerogels of high specific surface area prepared from nanofibrillated cellulose (NFC). Compos Sci Technol 71:1593–1599. https://doi.org/10.1016/j.compscitech.2011.07.003

[20] Li B, Yang X (2020) Rutin-loaded cellulose acetate/poly(-ethylene oxide) fiber membrane fabricated by electrospinning: a bioactive material. Mater Sci Eng C 109:110601. https://doi.org/10.1016/j.msec.2019.110601

[21] Liu J, Wang S, Jiang L, Shao W (2021) Production and characterization of antimicrobial bacterial cellulose membranes with non-leaching activity. J Ind Eng Chem 103:232–238. https://doi.org/10.1016/j.jiec.2021.07.041

[22] Alfahel R, Azzam RS, Hafiz M et al (2020) Fabrication of fouling resistant Ti3C2Tx (MXene)/cellulose acetate nanocomposite membrane for forward osmosis application. J Water Process Eng. 38:101551. https://doi.org/10.1016/j.jwpe.2020.101551

[23] Mahadik DB, Lakshmi RV, Barshilia HC (2015) High performance single layer nano-porous antireflection coatings on glass by sol–gel process for solar energy applications. Sol Energy Mater Sol Cells 140:61–68. https://doi.org/10.1016/j.solmat.2015.03.023

[24] Zhang F, Zhang WB, Shi Z, Wang D, Jin J, Jiang L (2013) Nanowire-haired inorganic membranes with superhydrophilicity and underwater ultralow adhesive superoleophobicity for high-efficiency oil/water separation. Adv Mater 25:4192–4198. https://doi.org/10.1002/adma.201301480

[25] Bharti B, Kumar S, Kumar R (2016) Superhydrophilic TiO_2 thin film by nanometer scale surface roughness and dangling bonds. Appl Surf Sci 364:51–60. https://doi.org/10.1016/j.apsusc.2015.12.108

[26] Wen Q, Di J, Jiang L, Yu J, Xu R (2013) Zeolite-coated mesh film for efficient oil–water separation. Chem Sci 4:591–595. https://doi.org/10.1039/C2SC21772D

[27] Qin A, Wu X, Ma B, Zhao X, He C (2014) Enhancing the antifouling property of poly(vinylidene fluoride)/SiO_2 hybrid membrane through TIPS method. J Mater Sci 49:7797–7808. https://doi.org/10.1007/s10853-014-8490-y

[28] Shen J-n, Ruan H-m, L-g Wu, Gao C-j (2011) Preparation and characterization of PES–SiO_2 organic–inorganic composite ultrafiltration membrane for raw water pretreatment. Chem Eng J 168:1272–1278. https://doi.org/10.1016/j.cej.2011.02.039

[29] Li J, Li D, Li W, Li H, She H, Zha F (2016) Facile fabrication of underwater superoleophobic SiO_2 coated meshes

for separation of polluted oils from corrosive and hot water. Sep Purif Technol 168:209–214. https://doi.org/10.1016/j.seppur.2016.05.053

[30] Wahid F, Zhao X-J, Duan Y-X, Zhao X-Q, Jia S-R, Zhong C (2021) Designing of bacterial cellulose-based superhydrophilic/underwater superoleophobic membrane for oil/water separation. Carbohydr Polym 257:117611. https://doi.org/10.1016/j.carbpol.2020.117611

[31] Mohammadkazemi F, Azin M, Ashori A (2015) Production of bacterial cellulose using different carbon sources and culture media. Carbohydr Polym 117:518–523. https://doi.org/10.1016/j.carbpol.2014.10.008

[32] Singhsa P, Narain R, Manuspiya H (2018) Physical structure variations of bacterial cellulose produced by different Komagataeibacter xylinus strains and carbon sources in static and agitated conditions. Cellulose 25:1571–1581. https://doi.org/10.1007/s10570-018-1699-1

[33] Sakthisabarimoorthi A, Martin Britto Dhas SA, Jose M (2018) Electrical impedance spectroscopic investigations of monodispersed SiO_2 nanospheres. Superlattices Microstruct 113:271–282. https://doi.org/10.1016/j.spmi.2017.11.001

[34] Cerveny S, Schwartz GA, Otegui J, Colmenero J, Loichen J, Westermann S (2012) Dielectric study of hydration water in silica nanoparticles. J Phys Chem C 116:24340–24349. https://doi.org/10.1021/jp307826s

[35] Chen Q, Ge Y, Granbohm H, Hannula S-P (2018) Effect of ethanol on Ag@Mesoporous silica formation by in situ modified Stöber method. Nanomaterials 8:362. https://doi.org/10.3390/nano8060362

[36] Yoo JW, Yun DS, Kim HJ (2006) Influence of reaction parameters on size and shape of silica nanoparticles. J Nanosci Nanotechnol 6:3343–3346. https://doi.org/10.1166/jnn.2006.006

[37] De G, Karmakar B, Ganguli D (2000) Hydrolysis–condensation reactions of TEOS in the presence of acetic acid leading to the generation of glass-like silica microspheres in solution at room temperature. J Mater Chem 10:2289–2293. https://doi.org/10.1039/b003221m

[38] Meškinis Š, Vasiliauskas A, Andrulevičius M, Peckus D, Tamulevičius S, Viskontas K (2020) Diamond like carbon films containing Si: structure and nonlinear optical properties. Materials 13:1003. https://doi.org/10.3390/ma13041003

[39] Lamastra FR, Mori S, Cherubini V, Scarselli M, Nanni F (2017) A new green methodology for surface modification of diatomite filler in elastomers. Mater Chem Phys 194:253–260. https://doi.org/10.1016/j.matchemphys.2017.03.050

[40] Wang Z, Ji S, He F, Cao M, Peng S, Li Y (2018) One-step transformation of highly hydrophobic membranes into superhydrophilic and underwater superoleophobic ones for high-efficiency separation of oil-in-water emulsions. J Mater Chem A 6:3391–3396. https://doi.org/10.1039/C7TA10524J

[41] Gao J, Cai M, Nie Z, Zhang J, Chen Y (2021) Superwetting PVDF membrane prepared by in situ extraction of metal ions for highly efficient oil/water mixture and emulsion separation. Sep Purif Technol 275:119174. https://doi.org/10.1016/j.seppur.2021.119174

[42] Ge J, Zong D, Jin Q, Yu J, Ding B (2018) Biomimetic and superwettable nanofibrous skins for highly efficient separation of oil-in-water emulsions. Adv Funct Mater 28:1705051. https://doi.org/10.1002/adfm.201705051

[43] Zhu Y, Zhang F, Wang D, Pei XF, Zhang W, Jin J (2013) A novel zwitterionic polyelectrolyte grafted PVDF membrane for thoroughly separating oil from water with ultrahigh efficiency. J Mater Chem A 1:5758–5765. https://doi.org/10.1039/C3TA01598J

[44] Shao L, Wang ZX, Zhang YL, Jiang ZX, Liu YY (2014) A facile strategy to enhance PVDF ultrafiltration membrane performance via self-polymerized polydopamine followed by hydrolysis of ammonium fluotitanate. J Membr Sci 461:10–21. https://doi.org/10.1016/j.memsci.2014.03.006

[45] Ong C, Shi Y, Chang J et al (2019) Tannin-inspired robust fabrication of superwettability membranes for highly efficient separation of oil-in-water emulsions and immiscible oil/water mixtures. Sep Purif Technol 227:115657. https://doi.org/10.1016/j.seppur.2019.05.099

[46] Zuo J-H, Cheng P, Chen X-F, Yan X, Guo Y-J, Lang W-Z (2018) Ultrahigh flux of polydopamine-coated PVDF membranes quenched in air via thermally induced phase separation for oil/water emulsion separation. Sep Purif Technol 192:348–359. https://doi.org/10.1016/j.seppur.2017.10.027

[47] Yu Q, Jiang Z, Yu Y et al (2021) Synchronous removal of emulsions and organic dye over palladium nanoparticles anchored cellulose-based membrane. J Environ Manage 288:112402. https://doi.org/10.1016/j.jenvman.2021.112402

[48] Liu Y, Wei R, Lin O et al (2017) Enhanced hydrophilic and antipollution properties of PES membrane by anchoring SiO_2/HPAN Nanomaterial. ACS Sustain Chem Eng 5:7812–7823. https://doi.org/10.1021/acssuschemeng.7b01304

[49] Cheng Q, Ye D, Chang C, Zhang L (2017) Facile fabrication of superhydrophilic membranes consisted of fibrous tunicate cellulose nanocrystals for highly efficient oil/water separation. J Membr Sci 525:1–8. https://doi.org/10.1016/j.memsci.2016.11.084

[50] Huang Y, Zhan H, Li D, Tian H, Chang C (2019) Tunicate cellulose nanocrystals modified commercial filter paper for efficient oil/water separation. J Membr Sci 591:117362. https://doi.org/10.1016/j.memsci.2019.117362

[51] Ao C, Zhao J, Li Q et al (2020) Biodegradable all-cellulose composite membranes for simultaneous oil/water separation and dye removal from water. Carbohydr Polym 250:116872. https://doi.org/10.1016/j.carbpol.2020.116872

[52] Zhou K, Zhang QG, Li HM, Guo NN, Zhu AM, Liu QL (2014) Ultrathin cellulose nanosheet membranes for superfast separation of oil-in-water nanoemulsions. Nanoscale 6:10363–10369. https://doi.org/10.1039/C4NR03227F

[53] Ao C, Zhao J, Xia T et al (2021) Multifunctional $La(OH)_3$@cellulose nanofibrous membranes for efficient oil/water separation and selective removal of dyes. Sep Purif Technol 254:117603. https://doi.org/10.1016/j.seppur.2020.117603

[54] Zhan H, Peng N, Lei X et al (2018) UV-induced self-cleanable TiO_2/nanocellulose membrane for selective separation of oil/water emulsion. Carbohydr Polym 201:464–470. https://doi.org/10.1016/j.carbpol.2018.08.093